

# Extraction of the Global Maximum Power for PV System under PSC Using an Improved PSO Technique

Claude Bertin Nzoundja Fapi<sup>1,2\*</sup>, Hyacinthe Tchakounté<sup>3,4</sup>, Martial Ndje<sup>5</sup>, Patrice Wira<sup>2</sup>, Martin Kamta<sup>3</sup>

<sup>1</sup> LS2N Laboratory, École Centrale de Nantes, Nantes University, 1 Rue de la Noë, 44321 Nantes, France

<sup>2</sup> IRIMAS Laboratory, University of Haute Alsace, 61 Albert Camus Road, 68093 Mulhouse, France

<sup>3</sup> LESIA Laboratory, ENSAI, University of Ngaoundéré, Ngaoundéré, P.O.B. 455, Cameroon

<sup>4</sup> LAMSEBP Laboratory, Faculty of Science, University of Yaoundé I, Yaoundé, P.O.B. 812, Cameroon

<sup>5</sup> Department of Electrical Engineering, Fotso Victor University Institute of Technology, University of Dschang, Bandjoun, P.O.B. 134, Cameroon

\* Corresponding author, e-mail: [nzoufaclauber@yahoo.fr](mailto:nzoufaclauber@yahoo.fr)

Received: 24 March 2023, Accepted: 28 July 2023, Published online: 28 September 2023

## Abstract

To get the most power out of photovoltaic (PV) panels, PV systems must utilize a maximum power point tracking (MPPT) controller. In partial shading conditions (PSC), the power-voltage (P-V) characteristic of the PV network may show a single global maximum power point (GMPP) and two or more local maximum power points (LMPP). This indicates that the PV cells and panels do not get uniform illumination. As they converge on the maximum power point (MPP) that makes contact first, which is often one of the LMPPs in this scenario, common MPPT approaches like incremental conductance (InC) and perturb and observe (P&O) are unable to distinguish between a GMPP and LMPPs. In this paper, the extraction of the GMPP of the PV system under PSC based on a suggested particle swarm optimization (PSO) approaches is presented. The particularity of the suggested approach is that it takes into account the calculation of the position of each particle as a function of the duty cycle and the global maximum power. Results on the performance of the suggested PSO method show an advantage over the conventional PSO and the commonly used traditional P&O method. The suggested PSO technique offer better performance in terms of global power extracted, ripple rate of the power and efficiency.

## Keywords

photovoltaic system, global maximum power point, partial shading conditions, particle swarm optimization

## 1 Introduction

Nowadays, the optimization of the photovoltaic (PV) modules performance is becoming more and more important because they exploit a renewable, modular and non-polluting energy [1]. The simplest and most economical way to improve the PV arrays is to add bypass diodes to the PV system. Then operate the system at its maximum power point (MPP) by combining a maximum power point tracking (MPPT) controller to the power electronic converter [2–4]. This solution remains incomplete due to the fact that there are always unpredictable shading sources but also due to the fact that it is necessary to rigorously choose an MPPT approach that is able to take into account the shading phenomenon while running the PV system at its maximum power [5].

A series of MPPT strategies have been realized in the literature to improve PV system performance. They can

be classified in several groups of classical techniques such as: hill climbing (HC) [6], incremental conductance (InC) [7, 8], perturb and observe (P&O) [9–11], fractional open circuit voltage (FOCV) [10] and fractional short circuit current (FSCC) [12] to name a few. In specifically, the P&O method makes use of a disturbance in the operational voltage of the PV system [9]. The main shortcomings of this approach, however, are the oscillations around the MPP, which is shown, and its limited ability to follow this point under cyclical environmental circumstances. Elgendy et al. [13] introduced the InC technique to lessen these oscillations and improve system efficiency; however it did not completely remove oscillations. Moreover, these systems need a series of procedures to choose the optimal duty cycle value, which might lead to inaccurate or slow

monitoring during sudden changes in temperature or irradiance [7]. Intelligent methods can also be mentioned to extract the MPP: the genetic algorithm (GA) [14], the Grey Wolf Optimizer (GWO) [14], the particle swarm optimization (PSO) [15–18], the fuzzy logic controller (FLC) [19, 20] and the artificial neural network (ANN) [21]. These algorithms provide a quicker time response and better stability under a variety of operating conditions because they employ a variable step to calculate the appropriate duty cycle value.

In the same vein, one of the biggest obstacles of solar panels is the partial shading conditions (PSC) that occurs when a part of the solar panel surface is no longer irradiated due to dust, an animal, or a surrounding mask. As a matter of fact, in PV arrays, the partial shading phenomenon not only leads to hot spots in PV modules but is also considered to be one of the main causes of PV systems energy efficiency reduction. Some authors have tried to solve this problem by modifying the PSO method or by combining it with other smart approaches [2–5]. Farh et al. [21] suggested a hybrid particle swarm optimization-fuzzy logic controller (PSO-FLC) algorithm for retrieving the overall PV system peak dynamically from the partially shaded system. This approach uses two PSO particle dispersing techniques capable of effectively solving the time invariance problem of PSO and the problem of strong oscillations around steady states. As a result, the latter approach will thus improve the performance of the PV system both under normal and PSC. In the same line of thought, Li et al. [15] improved the accuracy of the MPPT by proposing an overall distribution (OD) MPPT algorithm integrated in the PSO to rapidly search the area near the global maximum power points (GMPP). Hence the appellation OD-PSO MPPT algorithm, always with the aim of minimizing the monitoring time and increasing the yield of PV modules. Ibrahim et al. [22] suggested a cuckoo search algorithm (CS) for determination of GMPP of PV under PS. Ibrahim et al. [17] suggested an improved version of particle swarm optimization algorithm (IPSO) to solve the same problem. The fundamental difference between these last two works lies on practical application purpose. For instance, the last one is applied to a PV array functioning under PSC. In order to solve the problem of long convergence time, GP stored in memory, and the problem of sudden change of PSCs, a new rapid adaptive PSO (APSO) strategy has been proposed in [16]. Despite these previous works and the many algorithms developed, the problem of high MPPT tracking time and that of oscillations during the exploitation phase remain relevant. This

is how several works have been oriented in this direction this last years, the most important of which will be: the collaborative swarm algorithm (CSA) presented in [23] which is an association of three soft computing algorithms PSO, ACO-NUP, Jaya, and the cat swarm optimization (CSO) method presented in [24], the hybrid GWO sine cosine algorithm suggested in [25], and its improved version described in [26], to take into account the congestion cost of the electricity system and avoid being trapped in local optima. The hybrid MPPT algorithm (PSO+P&O and PSO+InC) presented in [27], which additionally varies the step size of conventional methods, InC and P&O in order to optimize the maximum PV output power. Some authors have been interested in finding reliable methods to assess the performance of different MPPT approaches. We can cite: the experimental technique for evaluating the adaptive tracking of the MPP for an autonomous PV system from Yadav et al. [14], the benchmark test from Javed and Ishaque [28] called RLD (length distribution runtime) to assess the effectiveness of several MPPT techniques inspired by evolutionary algorithms (EA) with various shaded curves.

The new method that is proposed in this work not only avoids the damage related to shading (destruction of solar cells, fires...), but also allows the PV system to operate at its overall maximum power. The particularity of the proposed approach is that it takes into account the calculation of the position of each particle as a function of duty cycle and the global maximum power. The remainder of this document is outlined as follows: Section 2 highlights the PV system configuration and its characteristics under PSC. Section 3 describes the process of extraction of the GMPP with an improved PSO approach. Section 4 highlights the results and an explanation of how the enhanced algorithm performed, and Section 5 concludes the work.

## 2 PV system characteristics under PSC

### 2.1 PV system configuration

Fig. 1 shows the schematic diagram of five PV modules connected in series under various types of partial shading. The solar PV panel used for this configuration is a Voltec Solar Tarka 60 [29]. Each PV panel generates a maximum voltage of 31.2 Volts and a maximum current of 8.7 Amps. The series connection of our system allows us to produce a power of 1357 Watts. This power supplies a load through a boost converter. The varied signals produced by the voltage and current are utilized by the MPPT algorithms to drive the boost converter in order to get the most power out of the solar system. At a constant temperature of 25 °C

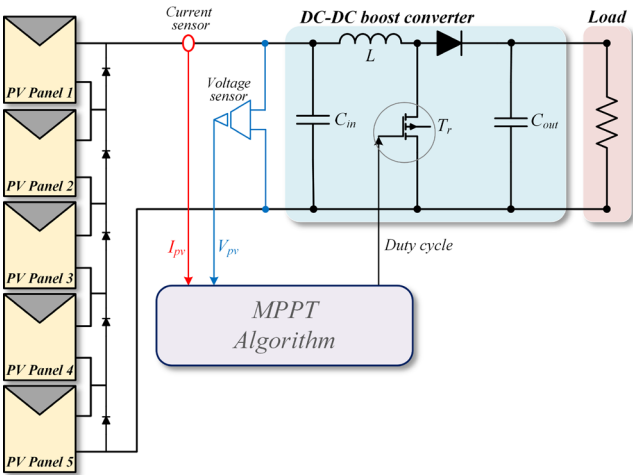


Fig. 1 Block diagram of five PV modules connected in series under different shading patterns

and during each second, the PSC are obtained by applying a various irradiance profile to each PV panel.

## 2.2 Solar cell modeling

The basic element of a PV generator is the solar cells, and its mathematical model is established by first finding its equivalent electrical circuit. Several models are published in the literature and tested under different conditions such as: the ideal model, the one-diode model, the two-diode model, the three-diode model and can be generated by the multi-dimensional diodes [1, 12, 18]. These models differ between them by the implementation procedure, the modeling and the number of parameters involved in the calculation of its power. They can also differ from the number of parameters in the electrical models. These models were developed to represent the highly nonlinear behavior of the semiconductor junction under variable solar radiation and temperature. It is then able to simulate PV behavior under hard climates such as arid or semi-arid conditions. A solar cell is an electronic circuit which, when illuminated by photons, generates electricity by PV effect. Fig. 2 depicts the corresponding single diode model of a solar cell.

Applying Kirchhoff's principles to the electric circuit of Fig. 2 yields Eq. (1) [12, 18], which describes the current generated by the solar cell:

$$I = I_{ph} - I_o \left[ \exp\left(\frac{V + R_s I}{nN_{sc} V_t}\right) - 1 \right] - \frac{V + R_s I}{R_p}, \quad (1)$$

where  $I$  (in Amps) and  $V$  (in Volts) indicate respectively the current at the output of the PV cell and the output voltage across it.  $I_{ph}$  and  $I_o$  are denoted the photo-generated current and the inverse saturation current of the diode respectively (in Amps).  $t$  is the temperature of the cell (in °C),  $n$  is the ideality factor of the diode.

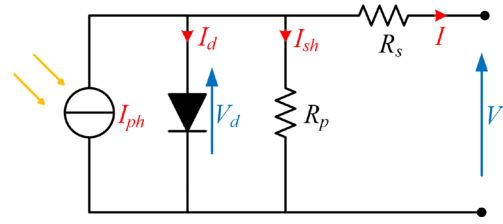


Fig. 2 The equivalent electrical model of a single diode solar cell

The value of the thermal voltage is given by Eq. (2):

$$V_t = \frac{kT}{q}, \quad (2)$$

where  $k$  and  $q$  (in Coulomb) indicate the Boltzmann constant and elementary charge or charge of the electron respectively.

The relationship given below defines the photo-generated current:

$$I_{ph} = \frac{G}{G_{ref}} \left[ I_{sc} + K_i (T - T_{ref}) \right], \quad (3)$$

where  $I_{sc}$  (in Amps) is the short-circuit current of the solar cell under standard test conditions (STC), which are: 25 °C and 1000 W/m<sup>2</sup>.  $T$  and  $T_{ref}$  referred to as the actual and the reference temperatures respectively (in °C).  $K_i$  is the current coefficient (in %/°C).  $G$  is the radiation on the PV surface and  $G_{ref}$  is the nominal radiation (generally  $G_{ref} = 1000$  W/m<sup>2</sup>).

The diode's inverse saturation current is defined as:

$$I_o = \frac{I_{sc} + K_i (T - T_{ref})}{\exp\left[\frac{V_{oc} + K_v (T - T_{ref})}{nN_{sc} V_t}\right] - 1}, \quad (4)$$

where  $V_{oc}$  (in Volts) and  $K_v$  (in %/°C) denote the open circuit voltage of the cell under reference case and the voltage coefficient respectively.

In this paper, the parameters values of the Voltec Solar Tarka 60 PV panel under the standard test condition are recapitulated in Table 1.

## 2.3 Characteristic of the partial shading system

In order for the high-power output required in some PV power generation systems to be achieved. Several PV modules must be linked in a string configuration (parallel, series, series-parallel etc.). In this configuration, not all PV panels are subject to the same atmospheric conditions (temperature and irradiance): this is called a PSC. When a PV panel receives less irradiance than the others, it absorbs the power produced by another and dissipates

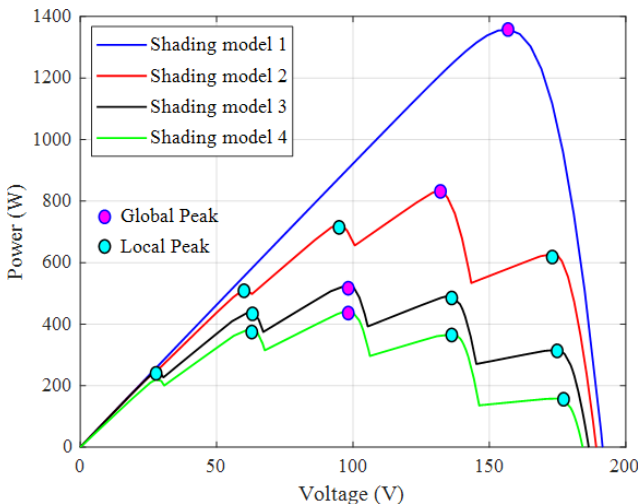
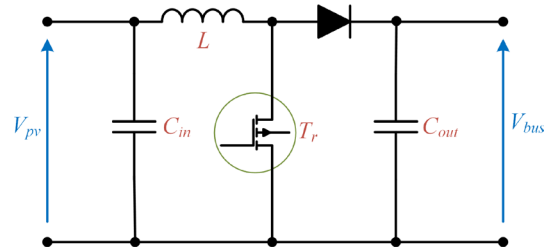
**Table 1** The voltec solar tarka 60 PV panel specifications at STC [29]

Parameters	Values	Symbols
Maximum power (W)	270	$P_{mpp}$
Maximum voltage (V)	31.2	$V_{mpp}$
Maximum current (A)	8.7	$I_{mpp}$
Open-circuit voltage (V)	38.3	$V_{oc}$
Short-circuit current (A)	9.3	$I_{sc}$
Temperature coefficient of $V_{oc}$ (%/°C)	-0.332	$k_{oc}$
Temperature coefficient of $I_{sc}$ (%/°C)	0.052	$k_{sc}$
Number of parallel cell	1	$N_p$
Number of series cells	72	$N_s$

heat; hence the sharp decrease in power obtained by all shaded PV modules. Under these conditions, we can observe on the trace of the power-voltage (P-V) features many points: several local maximum power points (LMPP) and one GMPP (see Fig. 3). Moreover, this operating point organizes its position according to the variations of the atmospheric conditions (sunlight and temperature). The characteristic curves of power versus voltage for the studied PV system for uniform irradiance and three shading models (SM) is indicated in Fig. 3. The PV system studied is obtained by combining five PV panels in series. The PSC patterns are respectively 950 W/m<sup>2</sup>, 850 W/m<sup>2</sup>, 400 W/m<sup>2</sup>, 700 W/m<sup>2</sup> and 1000 W/m<sup>2</sup> for case 1; 1000 W/m<sup>2</sup>, 800 W/m<sup>2</sup>, 600 W/m<sup>2</sup>, 400 W/m<sup>2</sup> and 200 W/m<sup>2</sup> for case 2; 900 W/m<sup>2</sup>, 700 W/m<sup>2</sup>, 500 W/m<sup>2</sup>, 300 W/m<sup>2</sup> and 100 W/m<sup>2</sup> for case 3.

## 2.4 Selecting Boost converter parameters

Fig. 4 depicts the corresponding circuit of the DC–DC boost converter. There are two modes of operation for the boost converter. First, the diode is blocked, and the switch  $T_r$  is unlocked ( $0 < t < dT$ ), at which point the current


**Fig. 3**  $P=f(V)$  specifications of the PV panels under PSC

**Fig. 4** Power circuit of the boost converter

in the boosting inductance grows linearly. The energy held in the inductor is evacuated to the output circuit through the diode when the switch  $T_r$  is secondarily locked ( $dT < t < T$ ) [1, 18]. This results in the formula shown below, where  $V_{pv}$  and  $V_{bus}$  stand for the input and output voltages of a boost converter, respectively:

$$V_{pv} = \frac{1}{1-\alpha} V_{bus}. \quad (5)$$

Equations (6) to (8) describe receptively the estimated inductor ( $\Delta I_L$ ), the inductance ( $L$  in Henry) and the capacitor ( $C$  in Farad) of the DC–DC boost converter:

$$\Delta I_L = \frac{V_{pv_{min}} \alpha}{f_s L}, \quad (6)$$

$$L = \frac{V_{pv} (V_{bus} - V_{pv})}{\Delta I_L f_s V_{bus}}, \quad (7)$$

$$C = \frac{I_{bus} \alpha}{f_s \Delta V_{bus}}, \quad (8)$$

where  $I_{bus}$  (in Amps) and  $f_s$  (in Hz) denote the output current and the switch frequency respectively,  $\Delta V_{bus}$  is the predicted output ripple voltage and  $V_{pv_{min}}$  is the minimum input voltage [1, 29].

In this study, the specifications values of the boost converter characteristics from Eq. (6), Eq. (7) and Eq. (8) are provided in Table 2.

## 3 Extraction of GMPP

Generally, an MPPT algorithm should be able to extract more power from a solar panel than the conventional power

**Table 2** Electrical specifications of the boost converter

Parameters	Values	Symbols
Switching frequency (KHz)	10	$f$
Input filter capacitor ( $\mu$ F)	34.856	$C_{in}$
Boost inductor ( $\mu$ H)	906.697	$L$
Output filter capacitor ( $\mu$ F)	216.576	$C_{out}$

converter. This is because MPPT algorithms can adjust the operating voltage and current of the panel to maximize the power output from the panel. In this heading, a proposed PSO method is presented. Then, its accuracy and performance are analyzed and accessed with conventional P&O and traditional PSO methods in Section 3.1.

### 3.1 Conventional P&O algorithm

The P&O technique is based on comparing the output power of a PV module with its prior disturbance cycle and periodically perturbing the voltage at the module's output [9–11]. The P&O MPPT command's flowchart is shown in Fig. 5 [9–11]. Two sensors are required to detect the current and voltage values in order to calculate the power at each instant. If the power diminishes for a voltage disturbance, the disturbance preserves its direction. If not, the equation is turned around such that the operational point moves closer to the MPP.

### 3.2 Conventional PSO

The social behavior of swarming animals such as flocks of birds was inspired by Kennedy and Eberhart in 1995 [15], thus allowing them to propose the technique called: PSO. The PSO is a meta-heuristic approach based on a population of simple agents, called particles [17]. Each particle, which has a starting location of  $x_i$  at time  $k$  and a velocity of  $v$ , cooperates and is regarded as a solution to the issue. Every particle also has a memory and can recall the best performance of both its position ( $p_{ibest}$ ) and that of other particles ( $g_{best}$ ). The displacement strategy of a particle in the PSO is illustrated in Fig. 6.

The PSO technique is mostly influenced by three factors: inertia, cognitive and social. In the inertia component, the particle tends to follow its current direction of

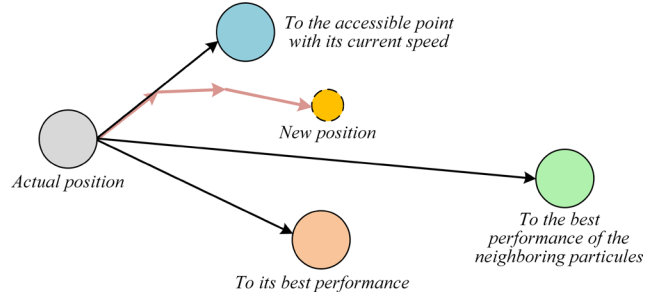


Fig. 6 Strategy for moving a particle in the PSO

travel. The cognitive component allows the particle to tend toward the best location. The particle moves and relies on the experience of its fellow particles and moves towards the best position already reached by the other particles thanks to the social component. The basic expression for the velocity of a particle is given by Eq. (9) [15–17, 28]:

$$v_i(k+1) = wv_i(k) + c_1r_1[p_{ibest} - x_i(k)] + c_2r_2[g_{best} - x_i(k)], \quad (9)$$

where  $w$  is the coefficient of inertia,  $c$  and  $r$  represent the acceleration coefficient and normalized random numbers in the interval  $[0, 1]$  respectively. Hence, the position update of a particle is given by Eq. (10):

$$x_i(k+1) = x_i(k) + v_i(k+1). \quad (10)$$

### 3.3 Improved PSO technique

The improved PSO technique in this work is based on an objective function for extracting the global maximum power in PV systems. This function consists of comparing the previous power value with the new value. The flowchart of the improved PSO is illustrated in Fig. 7. According to Fig. 7, the proposed PSO must satisfy Eq. (11):

$$D = f_{PSO}(V, I), \quad (11)$$

where  $V$  (in Volts) and  $I$  (in Amps) stand for the PV panel's voltage and current, respectively.

The steps of our flowchart are as follows: First of all, the initialization of the PSO specifications which are illustrated in Table 3. Secondly the particles are initialized by assigning the value zero to the components and new power vectors of the PV system through Eqs. (12) and (13):

$$P_{pv_o} = \text{zero}(1, \text{swarms}), \quad (12)$$

$$P_{pv_n} = \text{zero}(1, \text{swarms}). \quad (13)$$

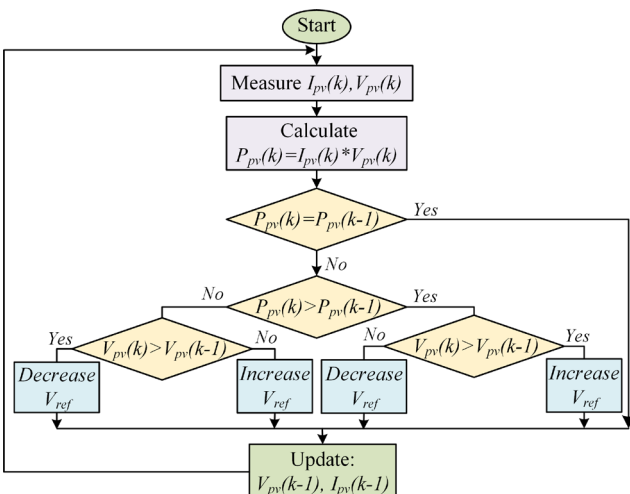


Fig. 5 The P&O algorithm flowchart

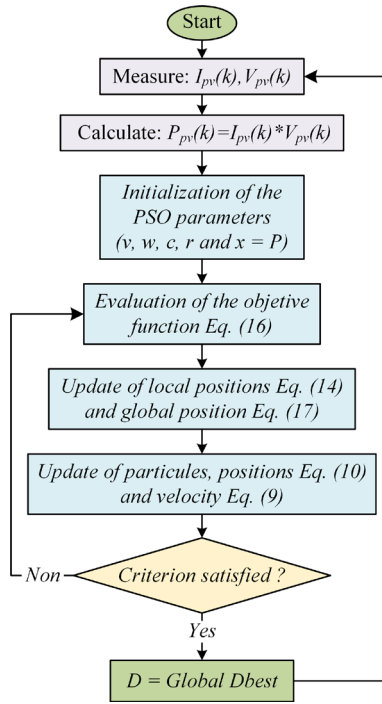


Fig. 7 Flowchart of an improved PSO algorithm

Table 3 Parameter used for the proposed PSO algorithm

Parameters	Values	Symbols
Number of swarms	10	<i>swarms</i>
Number of iterations	20	<i>iter<sub>max</sub></i>
Weight of local information	0.025	$c_1$
Global information weight	0.045	$c_2$
Weight of the inertia	0.4	$w$
Dimension of the problem	1	Dim
GMPP	0	GMPP

The positions of the particles ( $D_i$ ) are initialized by assigning them random values between 0 and 1 and to the components of position vectors which are those of the duty cycles as follows in Eq. (14):

$$D_i = w \times r(1, \text{swarms}). \quad (14)$$

The random initialization of the velocity is given by Eq. (15):

$$v_i = w \times r(1, \text{swarms}) \times [(V_{\max} - V_{\min}) + V_{\min}]. \quad (15)$$

The objective function in this approach is calculated according to Eq. (16):

$$P_{pv_o} = P_{pv_n}. \quad (16)$$

For a specific iteration and for each position,  $P_{pv_n}$  (in Watts) is calculated from the values of  $D_i$  and the new GMPP is determined. We therefore define the best

local duty cycle. Then, we check the new GMPP against the preceding GMPP in terms to Eq. (17):

$$\text{GMPP}_o = \text{GMPP}_n. \quad (17)$$

The first stopping criterion to be satisfied is based on Eq. (17). If  $\text{GMPP}_n$  is the same as  $\text{GMPP}_o$ , then the run point has achieved GMPP and the corresponding duty cycle ( $D$ ) is the equivalent of the best global duty cycle ( $\text{Global } g_{\text{best}}$ ). In order for the PSO algorithm to stop, the second condition is to reach the number of iterations without satisfying Eq. (17).

## 4 Results and discussion

The various components of Fig. 1 have been constructed and simulated using MATLAB/Simulink software [30] in order to assess the efficacy of the proposed PSO based MPPT approach. In Sections 4.1 and 4.2, we will respectively present the variations of the PSC used for each PV array. We will also present a detailed analysis of different MPPT algorithms based on simulation results.

### 4.1 PSC variation

PSC can vary depending on the time of day, the season, the location of the solar panel, the presence of nearby trees or animals, buildings, and other obstructions. In order to maximize solar energy gain, the solar panel should be positioned in an area that receives direct sunlight for the majority of the day and is not subject to significant shading. In this paper, the irradiance values of the five series-linked PV modules were found to be different, as given in Fig. 8. Partial shadowing conditions are achieved by pumping

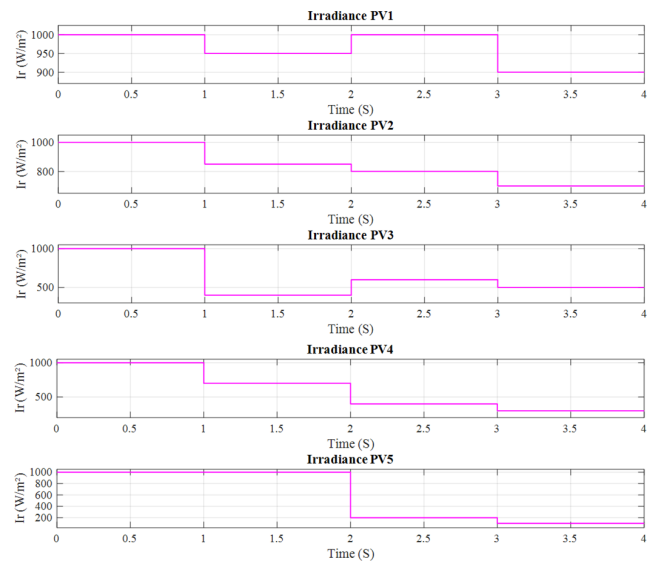


Fig. 8 Irradiance condition used for the PV string

multiple irradiance profiles into each PV module at a fixed temperature of 25 °C that change every one second.

The performance of a PV plant under different PSC can vary significantly. Different PSCs can affect the amount of energy produced, the efficiency of the system, and the reliability of the system. In this work, the four scenarios and the four models of PSC (SM1, SM2, SM3 and SM4) are indicated in Table 4. Each model is assigned to each PV module to analyze the behavior of the MPPT algorithms. For SM1, the irradiance on all PV modules is uniform; consequently, only one MPP peak appears on the current-voltage characteristic curve as shown in Fig. 3. For SM2, SM3 and SM4, there are respectively 4, 5 and 5 peaks. In addition, the values of current, voltage and power at the GMPPT for each model are shown.

#### 4.2 Performance of MPPT algorithms

The performance of a MPPT technique under PSC can be evaluated in terms of its ability to accurately track the MPP of a PV system. The MPPT technique should be able to accurately track the MPP of the PV system even under PSC, which can significantly reduce the overall efficiency of the system. MPPT performance under PSC can be evaluated in terms of the following parameters:

1. Tracking accuracy: This parameter measures the accuracy of the MPPT technique in tracking the MPP of the PV system under PSC. This is usually stated as a percentage of the total power provided by the PV system that is tracked by the MPPT technique.
2. MPPT speed: This parameter measures the speed at which the MPPT technique is able to track the MPP of the PV system under PSC. This is usually expressed as the time taken for the MPPT technique to adjust its tracking parameters to the new MPP.
3. Stability: This parameter measures the stability of the MPPT technique in tracking the MPP of the PV system under PSC.

To verify the ability of the proposed PSO-based MPPT approaches to track the GMPP, the PV system was emulated with various PSCs (SM2, SM4, and SM4) in addition to the standard test condition (SM1). The electrical

current and voltage curves provided by the PV system for the different optimization methods are presented in Fig. 9. In Fig. 9, we can see that the current and voltage at the PV output with the proposed PSO method are much more stable than those of the traditional P&O and conventional PSO, with ripple rates of 0.2 A and 0.2 V against 0.2 A and 0.2 V, and 5 A and 10 A respectively for those of the traditional P&O and conventional PSO: which proves the efficiency of the proposed PSO method.

The characteristic curves of the output power of the studied system with traditional P&O, conventional PSO and improved PSO algorithms are illustrated in Fig. 10(a).

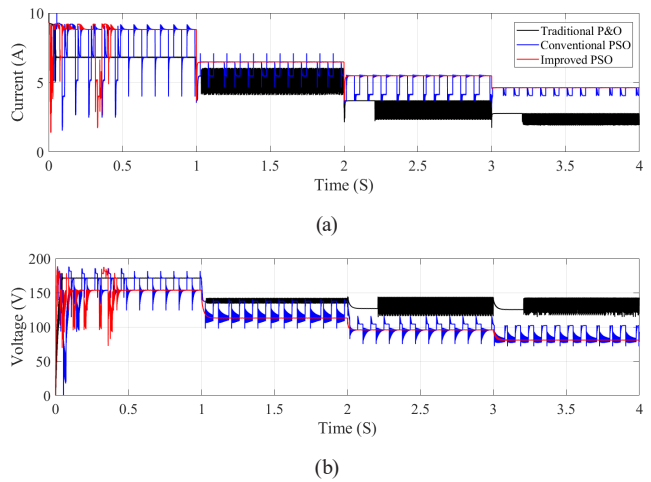


Fig. 9 Output curves of PV string for P&O, PSO and IPSO; (a) Current; (b) Voltage

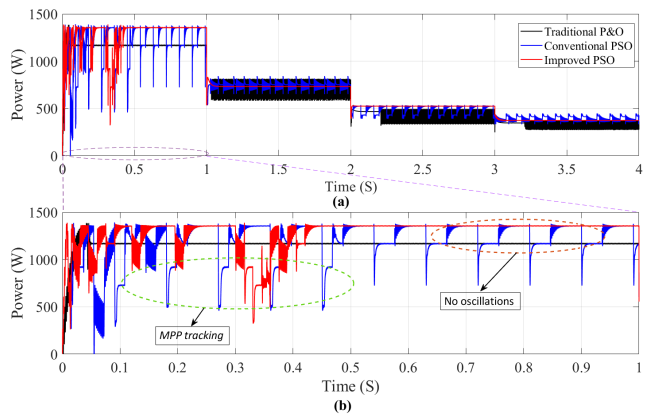


Fig. 10 Output curves of PV string for P&O, PSO and IPSO; (a) Power; (b) Zoom of power

Table 4 Global performance of PV plants under different PSC

Model	Time (s)	Partial shading scenario	$I_{mpp}$ (I)	$V_{mpp}$ (V)	$P_{mpp}$ (W)
SM1	[0, 1]	[1000, 1000, 1000, 1000, 1000]	8.7	156	1357
SM2	[1, 2]	[950, 850, 400, 700, 1000]	6.5	133	830
SM3	[2, 3]	[1000, 800, 600, 400, 200]	5.5	99	530
SM4	[3, 4]	[900, 700, 500, 300, 100]	4.5	99	440

After simulation under the conditions given in Section 4.1, it is clearly observed in Fig. 10(b) that the speed and stability of the PV power output of the suggested MPPT method is superior to those of the traditional methods. In addition, the output power peaks are suppressed hence the particle search sequence is optimized and consequently the power fluctuation is effectively reduced.

On one hand, from Fig. 10 and Table 5, the traditional P&O technique has low static settings, and its associated dynamic response is specialized in large fluctuations that disrupt the proper functioning of the PV system. On the other hand, the proposed PSO algorithm is able to track the GMPP correctly and dynamic performance is better than that of traditional P&O and conventional PSO in terms of stability efficiency and GMPP tracking when PSC occur.

The Traditional P&O, conventional PSO, and Enhanced PSO MPPT techniques performance analyses are indicated in Table 5. This table highlights that the proposed

approach is more suitable when the irradiance is important (SM1). Indeed, it offers the best maximum power, response time, efficiency, and ripple rate of the power. In addition, it should be noted that the response time is really very large and higher than for the conventional method for low Global Power extracted.

In Table 6, a summary of the performance parameters of the proposed PSO have been compared with the existing literature [15, 16, 18, 20, 22, 27, 28, 31–34]. The proposed PSO algorithm has been shown to outperform existing literature in terms of global performance, with a notable reduction in the number of iterations required to reach a solution. In particular, the PSO algorithm has been shown to converge faster than other EA such as GAs and ant colony optimization. Additionally, the PSO algorithm has been shown to be more accurate than other algorithms at finding the global optimum, while also requiring fewer evaluations of the objective function. Finally, the PSO algorithm has

**Table 5** Performance analysis of MPPT technique under PSC

?	Global power extracted $P_m$ (W)	MPPT techniques	Maximum power (W)	Response time $\tau_r$ (s)	Efficiency $\eta$ (%)	Ripple rate of the power $t_o$ (W)
SM1	1357	Traditional P&O	1150	0.05	84.47	1
		Conventional PSO	1262	1	92.99	10
		<b>Improved PSO</b>	<b>1352</b>	<b>0.2</b>	<b>99.63</b>	<b>0.2</b>
SM2	830	Traditional P&O	725	0.5	87.34	15
		Conventional PSO	820	0.5	98.79	5
		<b>Improved PSO</b>	<b>825</b>	<b>0.2</b>	<b>99.30</b>	<b>0.2</b>
SM3	530	Traditional P&O	500	1.5	94.33	10
		Conventional PSO	520	0.5	98.11	5
		<b>Improved PSO</b>	<b>525</b>	<b>0.2</b>	<b>99.05</b>	<b>0.2</b>
SM4	440	Traditional P&O	400	1.5	90.90	10
		Conventional PSO	425	0.5	96.59	5
		<b>Improved PSO</b>	<b>430</b>	<b>0.2</b>	<b>96.84</b>	<b>0.2</b>

**Table 6** Comparison of the suggested PSO's overall performance with current literature

Studies	Global Power extracted $P_m$ (W)	Maximum power (W)	Response time $\tau_r$ (s)	Efficiency $\eta$ (%)	Ripple rate of the power $t_o$ (W)
Present study	1357	1352	0.2	99.63	0.2
[31]	38.08	38.04	7.90	99.89	0.03
[15]	150	113.9	0.26	99.82	Not available (Na)
[22]	1319	1317.5	0.24	99.8	Na
[16]	175000	165800	3.3	99	0.02
[32]	97.7	92.4	0.1	94.57	0.7
[18]	90.2943	90.2913	0.2	99.99	0.5
[20]	98.85	98.7	0.15	99.8	Na
[33]	600	555	0.6	92.5	Na
[34]	10000	95460	0.4	94.99	0.5
[28]	1885	1619	0.3	98	0.3
[27]	100000	100300	0.0495	98.78	0.01



been demonstrated to produce better results than other algorithms in both low and high dimensional problems, allowing for a more efficient optimization of complex problems.

## 5 Conclusion

In this study, an improved PSO method for MPPT of a solar PV system under PSC has been developed. On the flip side, the suggested PSO performances have been compared with that of conventional P&O and PSO approaches. As the results, the proposed approach shows an interesting

global power extracted of 1352 W versus 1150 W and 1262.5 W for the traditional P&O and the PSO respectively. Furthermore, the suggested PSO technique increased the efficiency by 99.63%, which is an increase of 3% compared to the conventional PSO method. Finally, a better stability of the electric power is obtained in the presence of partial shading. The suggested method is therefore very suitable in a context where there is likely to be shading and where there are not very strong fluctuations in temperature. This stability is more pronounced for large values of irradiance.

## References

- [1] Nzoundja Fapi, C. B., Wira, P., Kamta, M. "A Fuzzy Logic MPPT Algorithm with a PI Controller for a Standalone PV System under Variable Weather and Load Conditions", In: 2018 International Conference on Applied Smart Systems (ICASS), Medea, Algeria, 2018, pp. 1–6. ISBN 978-1-5386-6867-2  
<https://doi.org/10.1109/icass.2018.8652047>
- [2] Yang, B., Zhu, T., Wang, J., Shu, H., Yu, T., Zhang, X., Yao, W., Sun, L. "Comprehensive overview of maximum power point tracking algorithms of PV systems under partial shading condition", Journal of Cleaner Production, 268, 121983, 2020.  
<https://doi.org/10.1016/j.jclepro.2020.121983>
- [3] Belhachat, F., Larbes, C. "A review of global maximum power point tracking techniques of photovoltaic system under partial shading conditions", Renewable and Sustainable Energy Reviews, 92, pp. 513–553, 2018.  
<https://doi.org/10.1016/j.rser.2018.04.094>
- [4] Sarvi, M., Azadian, A. "A comprehensive review and classified comparison of MPPT algorithms in PV systems", Energy Systems, 13(2), pp. 281–320, 2022.  
<https://doi.org/10.1007/s12667-021-00427-x>
- [5] Ali, A., Almutairi, K., Padmanaban, S., Tirth, V., Algarni, S., Irshad, K., Islam, S., Zahir, M. H., Shafiqullah, M., Malik, M. Z. "Investigation of MPPT techniques under uniform and non-uniform solar irradiation condition—A retrospection", IEEE Access, 8, pp. 127368–127392, 2020.  
<https://doi.org/10.1109/access.2020.3007710>
- [6] Nzoundja Fapi, C. B., Wira, P., Kamta, M., Badji, A., Tchakounte, H. "Real-time experimental assessment of hill climbing MPPT algorithm enhanced by estimating a duty cycle for PV system", International Journal of Renewable Energy Research (IJRER), 9(3), pp. 1180–1189, 2019.  
<https://doi.org/10.20508/ijrer.v9i3.9432.g7705>
- [7] Motahhir, S., El Hammoumi, A., El Ghzizal, A. "Photovoltaic system with quantitative comparative between an improved MPPT and existing INC and P&O methods under fast varying of solar irradiation", Energy Reports, 4, pp. 341–350, 2018.  
<https://doi.org/10.1016/j.egy.2018.04.003>
- [8] Huynh, D. C., Dunnigan, M. W. "Development and comparison of an improved incremental conductance algorithm for tracking the MPP of a solar PV panel", IEEE Transactions on Sustainable Energy, 7(4), pp. 1421–1429, 2016.  
<https://doi.org/10.1109/tste.2016.2556678>
- [9] Elgendy, M. A., Zahawi, B., Atkinson, D. J. "Assessment of perturb and observe MPPT algorithm implementation techniques for PV pumping applications", IEEE Transactions on Sustainable Energy, 3(1), pp. 21–33, 2012.  
<https://doi.org/10.1109/tste.2011.2168245>
- [10] Nzoundja Fapi, C. B., Kamta, M., Wira, P. "A comprehensive assessment of MPPT algorithms to optimal power extraction of a PV panel", Journal of Solar Energy Research, 4(3), pp. 172–179, 2019.  
<http://doi.org/10.22059/jsr.2019.287029.1126>
- [11] Guiza, D., Ounnas, D., Soufi, Y., Bouden, A., Maamri, M. "Implementation of Modified Perturb and Observe Based MPPT Algorithm for Photovoltaic System", In: 2019 1st International Conference on Sustainable Renewable Energy Systems and Applications (ICSRESA), Tebessa, Algeria, 2019, pp. 1–6. ISBN 978-1-7281-5357-5  
<https://doi.org/10.1109/icsresa49121.2019.9182483>
- [12] Nzoundja Fapi, C. B., Wira, P., Kamta, M., Tchakounté, H., Colicchio, B. "Simulation and dSPACE Hardware Implementation of an Improved Fractional Short-Circuit Current MPPT Algorithm for Photovoltaic System", Applied Solar Energy, 57(2), pp. 93–106, 2021.  
<https://doi.org/10.3103/S0003701X21020080>
- [13] Elgendy, M. A., Zahawi B., Atkinson D. J. "Assessment of the incremental conductance maximum power point tracking algorithm", IEEE Transactions on Sustainable Energy, 4(1), pp. 108–117, 2013.  
<https://doi.org/10.1109/tste.2012.2202698>
- [14] Yadav, K., Kumar, B., Guerrero, J. M., Lashab, A. "A hybrid genetic algorithm and grey wolf optimizer technique for faster global peak detection in PV system under partial shading", Sustainable Computing: Informatics and Systems, 35, 100770, 2022.  
<https://doi.org/10.1016/j.suscom.2022.100770>
- [15] Li, H., Yang, D., Su, W., Lü, J., Yu, X. "An Overall Distribution Particle Swarm Optimization MPPT Algorithm for Photovoltaic System Under Partial Shading", IEEE Transactions on Industrial Electronics, 66(1), pp. 265–275, 2019.  
<https://doi.org/10.1109/tie.2018.2829668>
- [16] Eltamaly, A. M., Al-Saud, M. S., Abokhalil, A. G., Farh, H. M. H. "Simulation and experimental validation of fast adaptive particle swarm optimization strategy for photovoltaic global peak tracker under dynamic partial shading", Renewable and Sustainable Energy Reviews, 124, 109719, 2020.  
<https://doi.org/10.1016/j.rser.2020.109719>

- [17] Ibrahim, A., Aboelsaud, R., Obukhov, S. "Improved particle swarm optimization for global maximum power point tracking of partially shaded PV array", *Electrical Engineering*, 101(2), pp. 443–455, 2019.  
<https://doi.org/10.1007/s00202-019-00794-w>
- [18] Hayder, W., Ogliari, E., Dolara, A., Abid, A., Ben Hamed, M., Sbita, L. "Improved PSO: a comparative study in MPPT algorithm for PV system control under partial shading conditions", *Energies*, 13(8), 2035, 2020.  
<https://doi.org/10.3390/en13082035>
- [19] Fapi, C. B. N., Wira, P., Kamta, M., Colicchio, B. "Design and hardware realization of an asymmetrical fuzzy logic-based MPPT control for photovoltaic applications", In: *IECON 2021 – 47th Annual Conference of the IEEE Industrial Electronics Society*, Toronto, ON, Canada, 2021, pp. 1–6. ISBN 978-1-6654-0256-9  
<https://doi.org/10.1109/IECON48115.2021.9589287>
- [20] Dehghani, M., Taghipour, M., Gharehpetian, G. B., Abedi, M. "Optimized Fuzzy Controller for MPPT of Grid-Connected PV Systems in Rapidly Changing Atmospheric Conditions", *Journal of Modern Power Systems and Clean Energy*, 9(2), pp. 376–383, 2021.  
<https://doi.org/10.35833/MPCE.2019.000086>
- [21] Farh, H. M. H., Eltamaly, A. M., Othman, M. F. "Hybrid PSO-FLC for dynamic global peak extraction of the partially shaded photovoltaic system", *PLoS One*, 13(11), e0206171, 2018.  
<https://doi.org/10.1371/journal.pone.0206171>
- [22] Ibrahim, A., Obukhov, S., Aboelsaud, R. "Determination of Global Maximum Power Point Tracking of PV under Partial Shading Using Cuckoo Search Algorithm", *Applied Solar Energy*, 55(6), pp. 367–375, 2019.  
<https://doi.org/10.3103/s0003701x19060045>
- [23] Deboucha, H., Shams, I., Belaid, S. L., Mekhilef, S. "A Fast GMPPT Scheme Based on Collaborative Swarm Algorithm for Partially Shaded Photovoltaic System", *IEEE Journal of Emerging and Selected Topics in Power Electronics*, 9(5), pp. 5571–5580, 2021.  
<https://doi.org/10.1109/jestpe.2021.3071732>
- [24] Nagadurga, T., Narasimham, P. V. R. L., Vakula, V. S. "Global Maximum Power Point Tracking of Solar Photovoltaic Strings under Partial Shading Conditions Using Cat Swarm Optimization Technique", *Sustainability*, 13(19), 11106, 2021.  
<https://doi.org/10.3390/su131911106>
- [25] Zafar, M. H., Khan, U. A., Khan, N. M. "Hybrid Grey Wolf Optimizer Sine Cosine Algorithm based Maximum Power Point Tracking Control of PV Systems under Uniform Irradiance and Partial Shading Condition", In: *2021 4th International Conference on Energy Conservation and Efficiency (ICECE)*, Lahore, Pakistan, 2021, pp. 1–6. ISBN 978-1-6654-4746-1  
<https://doi.org/10.1109/ICECE51984.2021.9406309>
- [26] Paul, K. "Modified grey wolf optimization approach for power system transmission line congestion management based on the influence of solar photovoltaic system", *International Journal of Energy and Environmental Engineering*, 13(2), pp. 751–767, 2022.  
<https://doi.org/10.1007/s40095-021-00457-2>
- [27] Ibrahim, M. H., Ang, S. P., Dani, M. N., Rahman, M. I., Petra, R., Sulthan, S. M. "Optimizing Step-Size of Perturb & Observe and Incremental Conductance MPPT Techniques Using PSO for Grid-Tied PV System", *IEEE Access*, 11, pp. 13079–13090, 2023.  
<https://doi.org/10.1109/access.2023.3242979>
- [28] Javed, S., Ishaque, K. "A comprehensive analyses with new findings of different PSO variants for MPPT problem under partial shading", *Ain Shams Engineering Journal*, 13(5), 101680, 2022.  
<https://doi.org/10.1016/j.asej.2021.101680>
- [29] Nzoundja Fapi, C. B., Wira, P., Kamta, M. "An Adaptive Fuzzy Logic Algorithm for Maximum Power Point Tracking under Partial Shading of a Solar Photovoltaic System", presented at *First International Conference on Energy Transition and Security (ICETS)*, Adrar, Algeria, July 28–30., 2021.
- [30] Mathworks "Implement PV array modules, (R2020a)", [computer program] Available at: <https://fr.mathworks.com/help/physmod/sps/powersys/ref/pvarray.html> [Accessed: 23 January 2022]
- [31] Sundareswaran, K., Vignesh Kumar, V., Palani, S. "Application of a combined particle swarm optimization and perturb and observe method for MPPT in PV systems under partial shading conditions", *Renewable Energy*, 75, pp. 308–317, 2015.  
<https://doi.org/10.1016/j.renene.2014.09.044>
- [32] Singh Chawda, G., Prakash Mahela, O., Gupta, N., Khosravy, M., Senju, T. "Incremental conductance based particle swarm optimization algorithm for global maximum power tracking of solar-PV under nonuniform operating conditions", *Applied Sciences*, 10(13), 4575, 2020.  
<https://doi.org/10.3390/app10134575>
- [33] Agrawal, P., Asim, M., Tariq, M. "Particle Swarm Optimization (PSO) for Maximum Power Point Tracking", In: *2022 2nd International Conference on Emerging Frontiers in Electrical and Electronic Technologies (ICEFEET)*, Patna, India, 2022, pp. 1–5. ISBN 978-1-6654-8876-1  
<https://doi.org/10.1109/icefeet51821.2022.9847759>
- [34] Dziri, S., Alhato, M. M., Bouallègue, S., Siarry, P. "Improved Particle Swarm Optimizer-Based MPPT Control of PV Systems Under Dynamic Partial Shading", In: *2022 19th International Multi-Conference on Systems, Signals & Devices (SSD)*, Sétif, Algeria, 2022, pp. 1603–1608. ISBN 978-1-6654-7109-1  
<https://doi.org/10.1109/ssd54932.2022.9955506>